Prediction of Effective Permittivity of Diphasic Dielectrics as a Function of Frequency

Marina Y. Koledintseva, Sandeep K. Patil, Robert W. Schwartz, Wayne Huebner
Missouri University of Science & Technology
1870 Miner Circle, Rolla, MO 65409, USA

Konstantin N. Rozanov
Institute for Theoretical and Applied Electromagnetics, Russian Academy of Sciences
13/19 Izhorskaya ul., Moscow, 125412, Russia

Jianxiang Shen, and **Ji Chen**
University of Houston, Department of Electrical and Computer Engineering, Houston, TX 77204, USA

ABSTRACT

An analytical model based on an equivalent impedance circuit for effective permittivity of a composite dielectric as a function of frequency with complex-shaped inclusions is presented. The geometry of the capacitor containing this composite dielectric is discretized into partial impedance elements, the total equivalent impedance is calculated, and the effective permittivity of the composite dielectric is obtained from this equivalent impedance. An example application using this method is given for an individual cell of a diphasic dielectric consisting of a high-permittivity spherical inclusion enclosed in a low-permittivity parallelepiped. The capacitance and resistance for individual discretized elements in the composite cell are modeled as a function of an inclusion radius. The proposed approach is then extended to a periodic three-dimensional structure comprised of multiple individual cells. The equivalent impedance model is valid for both static and alternating applied electric fields, over the entire range of volume fraction of inclusions. The equivalent impedance model has a few advantages over existing effective medium theories, including no limitations on the shape of inclusions or their separation distance.

Index Terms — **Dielectric composites, frequency, effective permittivity, equivalent impedance.**

1 INTRODUCTION

THEORETICAL efforts to predict the dielectric behavior of multiphase composites have been investigated for more than 100 years [1-5], and have resulted in a number of effective medium theories. The fundamental approach is to focus on one particular inclusion and then replace all of the rest by an effective homogenous medium. Any effective medium theory then is invariant to which particular inclusion is taken as a focus [6-9], since each inclusion must be surrounded by the same effective medium. One of the most widely-used formulations for calculating the effective permittivity of mixtures is the Maxwell Garnett (MG) theory [9-12]. MG theory is satisfactory when exact interparticle interactions are not significant, *i.e.*, for small concentrations (*inclusion volume fraction< 0.1*) of inclusions in a dielectric host [13]. The MG theory is applicable for inclusions of any arbitrary ellipsoidal shape, including spheres, spheroids, cylinders, and disks, through introducing depolarization factors [14]. Complex inclusion shapes can only be approximated by assuming a closest shape [15], which limits the overall applicability. The empirically derived logarithmic mixing rule is also widely applied for fitting experimental data [3]. However, the experimental fit of logarithmic mixing rule in some cases might be fortuitous, as was pointed out by Payne [16].

Properties of composite media have been intensively studied in the last two decades using various numerical techniques. The most prominent among these have been Monte Carlo simulations (MC) [17], the finite element method (FEM) [18, 19], the finite difference method [20]

Manuscript received on 28 May 2008, in final form 6 November 2008.

and the boundary integration method [21, 22]. It is noteworthy to consider the contribution of Sareni *et al.* who through use of numerical analysis techniques calculated the effective dielectric constant of periodic composites [21], random composites [23], and then also analyzed the complex effective permittivity of a lossy composite material [24]. Myroshnychenko et al [6] have developed an algorithm for predicting the complex permittivity of two-dimensional diphasic statistically isotropic heterostructures, and compared their results with different effective medium approaches.

Through numerical approaches it is possible in principle to study a system of any complexity, however, numerical analysis requires enormous computational resources that are costly and might not be always available.

The objective of this work was to obtain a simple closed-form analytical model that would allow for predicting the effective complex permittivities of diphasic composites. This model should be free from limitations on inclusion size and shape, as well as distances between inclusions. However, this model will remain in the quasistatic class, that is, sizes of inclusions will be much smaller compared to the corresponding wavelengths.

The model presented herein is based on discretization of a dielectric body into partial impedances, specifically, R-C elements, equivalent to "lossy capacitors." This can be applied to any inclusion shape. The effective permittivity is then calculated from the resultant impedance of the appropriate equivalent circuit. It should be mentioned that the analogous electric circuit approach was used by Pan et al [25] to predict the properties of a multilayer dielectric, with each single-phase layer having various grain sizes.

The approach presented herein has been applied to a high-permittivity inclusion in a low-permittivity host dielectric. As an example, the host dielectric is a parallelepiped (in particular, a cube). An inclusion in this example is a sphere, which is the simplest geometry to be compared with the MG theory and logarithmic mixing rule. This structure is referred to as "an individual cell" (or just "a cell"). The impedance of the cell is modeled as a function of an inclusion radius, or a volume fraction of an inclusion. The model is then extended to a composite three-dimensional (3D) structure comprised of periodically placed individual cells. Such a structure is found experimentally in systems as epoxy/$BaTiO_3$ [26-30].

It should be mentioned that the presented model considers only dielectric-dielectric mixtures, and only in quasistatic condition. There are known models, where the effective parameters of composites are considered based on equivalent circuits of inclusions, derived based on their polarizabilities [31, 32]. In these references, artificial magnetodielectrics are considered with conducting wire-shaped inclusions. The corresponding circuit models represent each inclusion as a radiating dipole, or a scatterer, so these are "antenna equivalent parameters" associated with plane wave exposure and scattering. This phenomenon is characteristic for metamaterials at very high, even optical frequencies. Radiation resistance of such "antennas" is different from ohmic loss, which is the only taken into account in our case.

Our case is different from [31, 32], since in our model we first assign equivalent capacitor model to a *diphasic dielectric structure*, and do not use polarizability. This is a comparatively low-frequency, quasistatic approach (unlike high-frequency up to optical band in considering metamaterials with artificial molecules). In our approach, the bulk of a capacitor individual cell is sliced into thin layers, each representing a partial capacitor, and this approach would be valid at dc. As frequency of voltage applied to the electrodes of the capacitor increases, some loss due to polarization of dielectric and very small conductivity current due to impurities in phases would appear and affect frequency response of the composite material.

2 MODEL DESCRIPTION

2.1 ONE INDIVIDUAL IMPEDANCE CELL (SPHERICAL INCLUSIONS)

A general diphasic slab with a three-dimensional periodic structure of inclusions is subdivided into individual cells (cubes), each containing one high-permittivity inclusion surrounded by a lower permittivity host material. Figure 1 shows the basic building block of the composite and its three-dimensional translation. First consider an individual cell with an inclusion of an isotropic shape, i.e., a sphere, placed at the center of a cube. The inclusion and the host are assumed to be linear isotropic and homogeneous dielectric materials, with an alternating electric field applied along the vertical dimension of the cell. In this case, any cell is simply an individual capacitor with an inhomogeneous dielectric inside, and can be discretized into parallel and series parallel-plate partial impedances, each containing a homogeneous dielectric. Figure 2a shows, how this structure is discretized into partial elements. Each element has its own impedance, in which a partial capacitor is parallel to the corresponding partial resistor, responsible for loss. The equivalent circuit corresponding to an individual cell is shown in Figure 2b. The total equivalent reactance, X_{eq}, and impedance, Z_{eq}, of the individual cell are

$$X_{eq} = \frac{1}{j\omega C_{eq}} \tag{1}$$

$$Z_{eq} = \frac{R_{eq} \cdot X_{eq}}{(R_{eq} + X_{eq})} \tag{2}$$

where R_{eq} and C_{eq} are the equivalent resistance and capacitance of the structure.

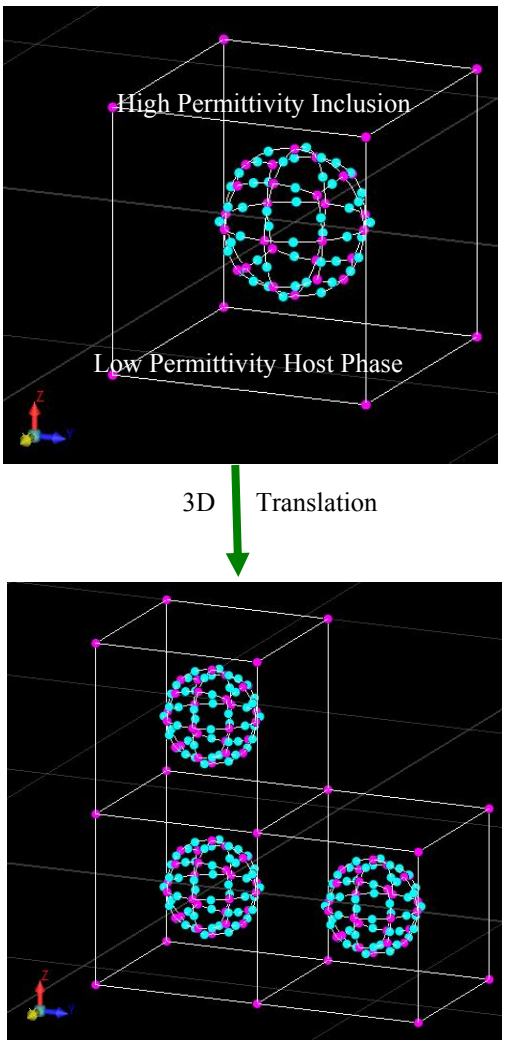

Figure 1. Basic building block of composite sphere enclosed in a cube and its 3-D translation in x, y, z directions.

The equivalent capacitance parallel-plate capacitor filled by effective dielectric medium is,

$$C_{eq} = \frac{Z''_{eq}}{\omega(Z'_{eq} + Z''_{eq})} \tag{3}$$

where ω is frequency of alternating electric field and Z'_{eq} and Z''_{eq} are real and imaginary parts of impedance, respectively.

Figure 3 shows the planar projection of the 3D view presented in Figure 2a. Z_1 and Z_2 are the impedances that are present on left and right hand side of the inclusion sphere.

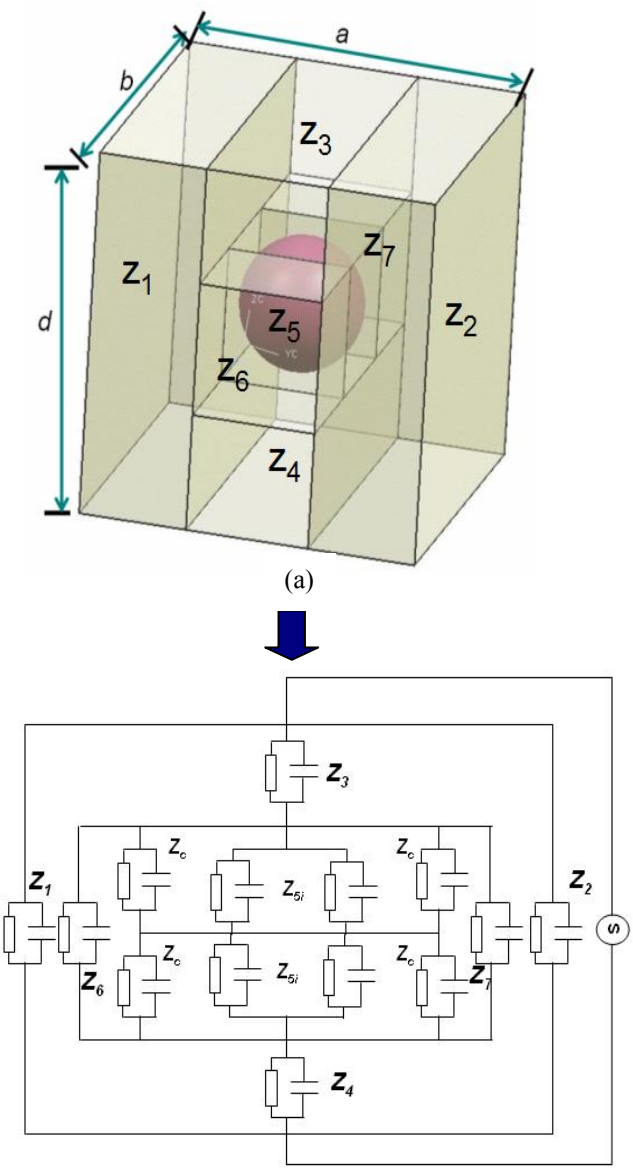

Figure 2. 3-D view of the discretized diphasic dielectric body and its corresponding equivalent circuit.

Assuming the structure is symmetrical, the capacitances C_1 and C_2 are

$$C_1 = C_2 = \frac{\varepsilon_0 \varepsilon_h (a_c / 2 - r) b_c}{d_c} \tag{4}$$

where ε_h is the relative permittivity of the host material. These capacitances linearly decrease as the radius of the inclusion increases.

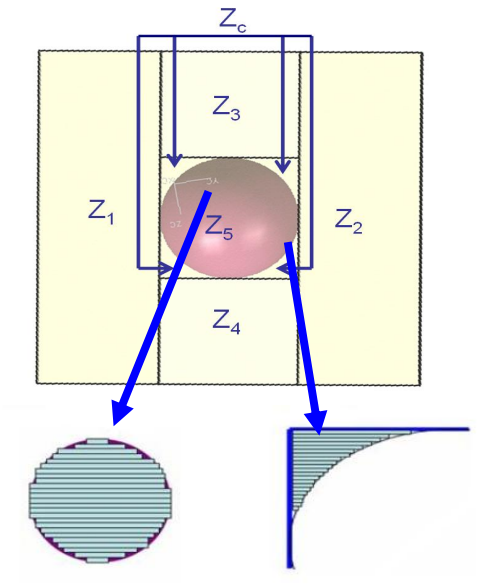

Figure 3. 2-D view of the discretized diphasic dielectric body and discretization pathway of corner shape and inclusion sphere.

The corresponding reactance for any α-th element is $X_\alpha = \dfrac{1}{j\omega C_\alpha}$. If the loss in the host material due to impurities is taken into account, then the resistances of each element are

$$R_1 = R_2 = \frac{2d_c}{\sigma_h (a_c - 2r) b_c} \tag{5}$$

where σ_h is the d.c. effective conductivity of the host; a_c, b_c, and d_c are the dimensions of the individual cell (in a particular case of a cube, $a_c = b_c = d_c$), and r is the radius of the inclusion.

It should be mentioned that loss in the host matrix, which may be a lossy polymer in general case, in our model may be taken into account not just as an effective conductivity, but through the host material frequency dependence, such as Debye, Cole-Cole, Cole-Davidson, or other model. Then it is more convenient to deal with conductances G_α, rather than resistances R_α, where α are the corresponding indices for partial elements of the equivalent circuit. Then capacitances are determined by the real part of the permittivity of the host matrix, and conductances depend on the imaginary part of permittivity. In this case it is more convenient to consider the equivalent circuit in terms of admittances, as done below in the section 2.3 regarding cylindrical inclusions.

The partial capacitances C_3 and C_4 and partial resistances R_3 and R_4 are the elements located on the top and the bottom of the inclusion, respectively, and are calculated as

$$C_3 = C_4 = \frac{4\varepsilon_0 \varepsilon_h b_c r}{d_c - 2r} \tag{6}$$

$$R_3 = R_4 = \frac{(d_c - 2r)}{4 \cdot r \cdot \sigma_h b_c} \tag{7}$$

The partial capacitances C_6 and C_7 and partial resistances R_6 and R_7, located in front of and behind the sphere (see Figure 2(a)), are calculated as

$$C_6 = C_7 = \frac{\varepsilon_0 \varepsilon_h (b_c - 2r)}{2} \tag{8}$$

$$R_6 = R_7 = \frac{2}{\sigma_h (b_c - 2r)} \tag{9}$$

Figure 3 shows the discretization pathway for the corner shape and inclusion sphere. The same discretization is adopted for calculating both partial capacitances and resistances. The resistance and capacitance of the corner elements are calculated using smaller discretization into elemental slices parallel to the electrode planes of the cell. They are connected in series, and the integration over the corner space is accomplished. The calculation of capacitance of corner capacitor elements and the inclusion sphere have been presented by Patil et al [33]. The detailed calculation of the resistance of the corner element is presented in the attached *Appendix A*. The total resistance and capacitance for all four corner elements- two bottom and two top $(i = 1...4)$ are

$$C_c = C_{c_i} = 2.76\varepsilon_0 \varepsilon_h r \tag{10}$$

$$R_c = R_{c_i} = \frac{1.326}{\sigma_h r} \tag{11}$$

To calculate the capacitance of the high-permittivity sphere, it is convenient to cut it into thin parallel slices, and consider series connection of the elements. The integration procedure yields the capacitance of the quarters of the dielectric sphere C_{5_i}, $(i = 1...4)$ which is the same as of the total sphere

$$C_5 = C_{5_i} = \frac{\varepsilon_0 \varepsilon_i \pi \cdot r}{2 \int_0^{\pi/2} \dfrac{d\theta}{\cos(\theta)}} \tag{12}$$

To assure convergence of the integral in the denominator, zero in the integration was substituted by 10^{-7}. The resistance of the inclusion sphere is calculated by first calculating the conductance of the sphere as shown below.

$$G_{5_i} = \frac{C_{5_i} \cdot \omega \cdot \varepsilon^{''}}{\varepsilon^{'}} \Rightarrow R_5 = R_{5_i} = \frac{1}{G_{5_i}} \tag{13}$$

The real and imaginary parts of the inclusion phase permittivity are calculated using the Debye expression

$$\varepsilon_i(\omega) = \varepsilon_{\infty i} + \frac{\varepsilon_{si} - \varepsilon_{\infty i}}{1 + j\omega\tau_i} \tag{14}$$

The impedance of any partial element with an index α is calculated as an impedance of parallel resistive element R_α and the reactive element X_α, connected in parallel

$$Z_\alpha = \frac{X_\alpha \cdot R_\alpha}{X_\alpha + R_\alpha} \tag{15}$$

The impedance of the central part of the equivalent circuit is

$$Z_{central} = Z_3 + Z_4 + \frac{1}{\frac{1}{Z_6} + \frac{1}{Z_7} + \frac{1}{\frac{Z_c Z_5}{Z_c + Z_5}}} \tag{16}$$

Finally, the equivalent impedance of the cell can be found as

$$Z_{eq} = \frac{1}{\frac{1}{Z_1} + \frac{1}{Z_2} + \frac{1}{Z_{central}}} \tag{17}$$

Since this equivalent impedance is comprised of equivalent capacitance and equivalent resistance elements connected in parallel, the values R_{eq} and C_{eq} can be obtained from the real and imaginary parts of $Z_{eq} = Z'_{eq} - jZ''_{eq}$. The equivalent capacitance of the individual cell is

$$C_{eq} = \frac{Z''_{eq}}{\omega \cdot (Z'^{\,2}_{eq} + Z''^{\,2}_{eq})} \tag{18}$$

Then, assuming that the homogeneous dielectric with permittivity $\varepsilon^{'}_{eff}$ fills the space between the cell capacitor plates, the real part of the effective permittivity is

$$\varepsilon'_{eff} = \frac{C_{eq} d_c}{\varepsilon_o a_c b_c} \tag{19}$$

By utilizing the equivalent impedance approach, $\varepsilon^{'}_{eff}$ and ε''_{eff} can be found as shown below. The effective permittivity (ε'_{eff}) captures the shape of the inclusion, and there are no restrictions on the inclusion size. Thus from the equivalent capacitance, the effective static permittivity can be found.

The equivalent resistance of the individual cell is

$$R_{eq} = \frac{Z'^{\,2}_{eq} + Z''^{\,2}_{eq}}{Z'_{eq}} \tag{20}$$

The equivalent conductance of the individual cell is simply the inverse of the equivalent resistance,

$$G_{eq} = \frac{1}{R_{eq}} \tag{21}$$

The imaginary part of the effective permittivity can be calculated from the equivalent conductance.

$$\varepsilon^{''}_{eff} = \frac{\varepsilon^{'}_{eff} \cdot G_{eq}}{\omega \cdot C_{eq}} \tag{22}$$

2.2 N^3 INDIVIDUAL IMPEDANCE CELL

Herein, a case with N spherical inclusions along each of the three dimensions of the total capacitor, resulting in N^3 individual cells, is considered. If the dimensions of the total capacitor are $a, b,$ and d, then the dimensions of an individual cell are

$$a_c = a/N, b_c = b/N, \text{and } d_c = d/N, \tag{23}$$

respectively.

The equivalent circuit of the total impedances contains individual cells in vertical branches connected in series, while all the branches are connected in parallel, as is shown in Figure 4. This means that the total equivalent impedance of all the branches is

$$Z_{eq} = \frac{Z_{branch}}{N^2} = \frac{Z_{cell}}{N} \tag{24}$$

Then the effective permittivity of an inhomogeneous dielectric inside the total capacitor can be calculated using equations (17) and (24) for ε'_{eff} and ε''_{eff}, respectively.

The effective permittivity of an inhomogeneous dielectric obtained using the method presented above is compared later on with the well-known homogenization technique based on the Maxwell Garnett (MG) mixing rule [9-12, 14] and logarithmic mixing rule [15]. For a mixture of a host material with relative permittivity ε_h and

spherical inclusions with relative permittivity ε_i , the Maxwell Garnett mixing rule is

$$\varepsilon_{eff\ MG} \cong \varepsilon_h + \frac{3 f_{vi} \varepsilon_h (\varepsilon_i - \varepsilon_h)/(\varepsilon_i + 2\varepsilon_h)}{1 - f_i (\varepsilon_i - \varepsilon_h)/(\varepsilon_i + 2\varepsilon_h)} \qquad (25)$$

where $f_{vi} = \frac{V_i}{V_\Sigma}$ is the volume fraction of spherical inclusions in the total mixture. Here V_i represents volume of inclusion and V_Σ represents volume of composite.

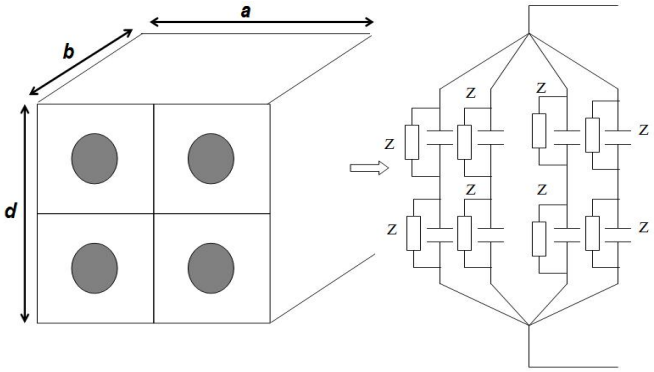

Figure 4. Discretization pathway for N^3 impedances.

The formulation for logarithmic mixing rule is given by

$$\varepsilon_{eff\ Logarithmic} \cong V_h \cdot \log \varepsilon_h + V_i \log \varepsilon_i \qquad (26)$$

Herein, V_h and ε_h is the volume fraction and permittivity of the host phase respectively. Also, V_i and ε_i is volume fraction and permittivity of the inclusion phase respectively.

2.3 INCLUSIONS OF CYLINDRICAL SHAPE

The similar equivalent impedance model can be applied to inclusions of any shape. For example, let us consider cylindrical high-permittivity inclusions embedded in a low-permittivity host. First consider an individual cell, comprised of a vertically placed cylinder at the center of a cube, as is shown in Figure 5.

The cube has dimensions $a \times b \times d$, as before. The height of the cylinder is h, and its radius is r. For every cylinder one can introduce its aspect ratio $A_{cyl} = h/(2r)$. The equivalent circuit is shown in Figure 6.

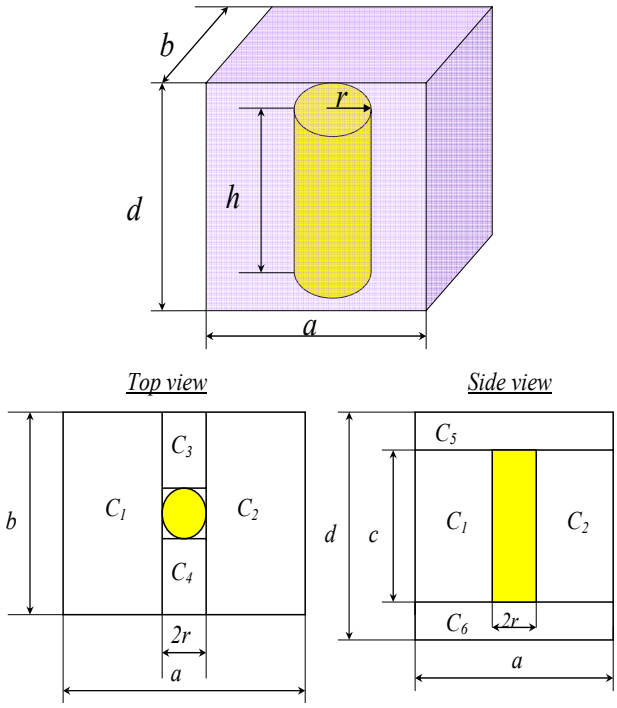

Figure 5. Cylindrical inclusion in a host cube and discretization for partial capacitors.

For the symmetrical location of the cylinder inside the host cube, the partial capacitances are

$$C_1 = C_2 = \frac{\varepsilon_0 \varepsilon_h (a - 2r) b}{2h}$$
$$C_3 = C_4 = \frac{\varepsilon_0 \varepsilon_h r (b - 2r)}{h}$$
$$C_5 = C_6 = \frac{2\varepsilon_0 \varepsilon_h ab}{d - h} \qquad (27)$$
$$C_{cyl} = \frac{\varepsilon_0 \varepsilon_i \pi r^2}{h}$$
$$C_{corner} = \frac{\varepsilon_0 \varepsilon_h (4r^2 - \pi r^2)}{4h}$$

The central part of the equivalent circuit would have the capacitance

$$C_{central} = C_{cyl} + 2C_1 + 2C_3 + 4C_{corner} \qquad (28)$$

and the equivalent capacitance of the total cell will be

$$C_\Sigma = \frac{C_5^{\,2} C_{central}}{C_5^{\,2} + 2C_5 C_{central}} \qquad (29)$$

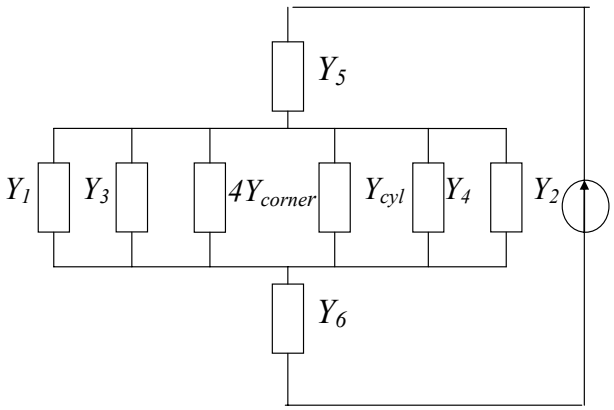

Figure 6. Equivalent circuit for a cylindrical inclusion in a host matrix.

However, this is a static capacitance without any loss. Loss in the circuit can be taken into account through the complex admittance for every element with index "*n*"

$$Y_n = j\omega C_n + G_n , \tag{30}$$

with a partial conductance

$$G_n = \frac{\omega C_n \varepsilon_n''}{\varepsilon_n'} \tag{31}$$

corresponding to every *n*-th element of the circuit with its own dielectric properties – either host or inclusion.

The central admittance will be

$$Y_{central} = 2Y_1 + 2Y_3 + 4Y_{corner} + Y_{cyl} \tag{30}$$

Then the resultant complex equivalent admittance is calculated as

$$1/Y_{eq} = 1/Y_{central} + 2/Y_5 \tag{31}$$

and its real and imaginary parts give equivalent conductance and capacitance.

$$\begin{aligned} G_{eq} &= \mathrm{Re}(Y_{eq}) \\ C_{eq} &= \mathrm{Im}(Y_{eq})/\omega \end{aligned} \tag{32}$$

Then the real part of the effective permittivity is calculated as

$$\varepsilon_{eff}' = \frac{C_{eq} d}{\varepsilon_0 ab} \tag{33}$$

and the imaginary part is calculated as

$$\varepsilon_{eff}'' = \frac{G_{eq}\varepsilon_{eff}'}{\omega C_{eq}} . \tag{34}$$

If the cube is subdivided in N^3 smaller cells, the equivalent circuit will contain N^2 parallel similar branches of N series elements, so that the admittance of the total circuit will not change. Therefore, the effective parameters can still be calculated using equations (33) and (34). Some results of calculations using this approach for cylindrical inclusions with different sizes and aspect ratios will be shown in the next section of the paper.

3 RESULTS AND DISCUSSION

Computations of the complex effective permittivity of a composite based on the equivalent RC circuit model are presented herein.

3.1 MIXTURE WITH INCLUSIONS OF SPHERICAL SHAPE

The 3D model is set up to mimic the real world system of a high permittivity phase inclusion in a polymeric host (ceramic - polymer composite) with 0-3 connectivity. Two cases have been investigated: the first with just one inclusion in the host matrix, and the second with 1000 inclusions inside the cube.

The experimental data for computations is taken from the paper of M.P. McNeal et al [34] which presented the microwave behavior of $BaTiO_3$, which can be approximated using the Debye frequency dependence [35],

$$\varepsilon_i(\omega) = \varepsilon_{\infty i} + \frac{\varepsilon_{si} - \varepsilon_{\infty i}}{1 + j\omega\tau_i} \tag{27}$$

In McNeal et al [34], the static permittivity for a coarse-grain $BaTiO_3$ ceramic is reported to be ε_{si}=1900, the "optical limit" permittivity is $\varepsilon_{\infty i}$=280, and the Debye constant is τ_i = 2.06 ns, which corresponds to a relaxation frequency $f_{ri} = \frac{\omega_{ri}}{2\pi}$ = 771 MHz. The host is assumed to be a low-loss dielectric, whose real part of relative permittivity is taken as ε_h = 4, and an effective ohmic conductivity in these computations is taken, for example, as σ_h = $3.79\cdot10^{-12}$ S/m (this value corresponds to glass). If the host material is a comparatively low-lossy polymer, its loss tangent $\tan\delta$ would be on the order of 10^{-3}…10^{-5}, depending on frequency in the microwave range. The dielectric cube surrounding one ceramic sphere (or multiple spheres) has the following dimensions: $a_c = b_c = d_c = 1.1$ μ m. The radius of the sphere is a varying parameter, and,

hence, the volume fraction of the inclusion or inclusions is also varying.

Figure 7a depicts the equivalent capacitance of the dielectric composite as a function of frequency and inclusion volume fraction. The inclusion volume fractions chosen were 2.5%, 8.4%, 20.1%, 39.3% and 46.8%, respectively. The equivalent capacitance as a function of inclusion volume fraction is dominated by the capacitor elements C_5, C_3 and C_4. As the volume fraction of the inclusion phase increases from 2.5% to 46%, the contribution of capacitor elements C_5, C_3 and C_4 increase due to the concurrent increase in area of the capacitor elements and decrease in the thickness of the host.

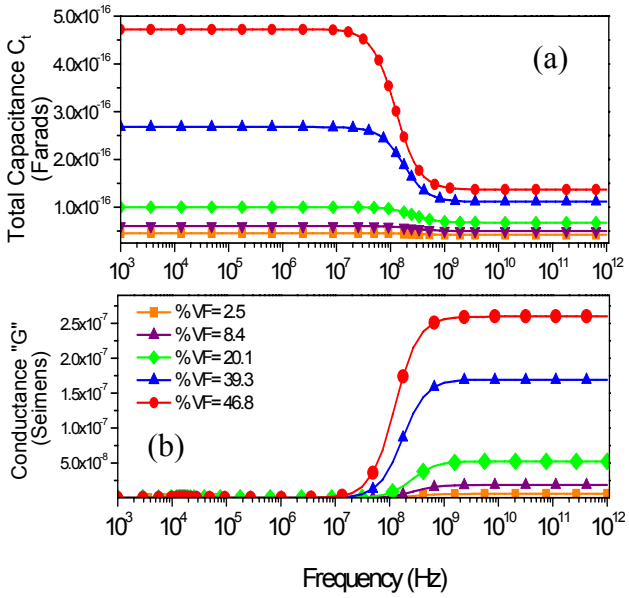

Figure 7. Magnitude of the equivalent capacitance and equivalent conductance of composite as a function of frequency and inclusion volume fraction.

It is known that as the frequency increases beyond the relaxation frequency, there is a decrease of dipolar and space charges, which results in the decrease of charge formed on capacitor plates, leading to the reduction in the equivalent capacitance. Figure 7a demonstrates this effect.

In Figure 7b, the equivalent conductance of the dielectric composite is plotted as a function of frequency. To understand the results generated by the analytical model, it is imperative to understand the physical response of a dielectric to an applied field as a function of frequency. As capacitors "conduct" current in proportion to the rate of voltage change, they will pass more current for faster-changing voltages (as they charge and discharge to the same voltage peaks in shorter time interval), and less current for slower-changing voltages. Therefore there would be an increase in the effective conductivity of the dielectric for frequencies above the relaxation frequency for all inclusion volume fractions. It is also seen from Figure 7b that with the increase in the volume fraction of the high-permittivity inclusion phase, the equivalent resistance decreases, and the equivalent conductance of the composite dielectric increases.

Figure 8 depicts the response of effective permittivity (ε'_{eff}) of the dielectric composite as a function of frequency. Figure 6 shows very clearly relaxation in dielectric properties. The real part of permittivity predicted by the equivalent impedance model at 10^3 Hz is $\varepsilon'_{eff} \approx 47$, and it decreases to ~11 at 10^{12} Hz, so that the difference $\Delta\varepsilon_{eff} = \varepsilon'_{eff\,s} - \varepsilon'_{eff\,\infty}$ (dielectric relaxation strength) is about 35. The ε'_{eff} remains essentially flat up to ~ 10^7 Hz, and above this frequency it decreases and follows the Debye frequency dependence. This prediction is for the highest inclusion volume fraction of 46.8 %. With the reduction of inclusion volume fraction to 39.3%, the effective permittivity ε'_{eff} of the composite reduced to 27 at 10^3 Hz and saturated to around 10^{12} Hz and yielding $\Delta\varepsilon_{eff} \approx 17$. $\Delta\varepsilon_{eff}$ continues to decrease with the inclusion volume fraction decrease, and this is an expected result as dispersive phase's volume fraction decreases in the non-dispersive host phase. All these predictions of permittivity were for a single inclusion in the host phase.

The dielectric relaxation in $BaTiO_3$ takes place at 771 MHz [34]. The frequency dependence of ferroelectricity including apparent disappearance of ferroelectric response in the microwave regions has been explained by von Hippel [36]. For a ferroelectric material like $BaTiO_3$, there are permanent electric dipoles which are firmly anchored into position and not available for free rotation. They are unable to follow the applied field at frequencies above the relaxation frequency, and this causes the decrease in the permittivity, as the contribution of dipolar polarization is no longer there. Another interesting observation can be made on examination of Figure 8. The characteristic peak of the imaginary part of the composite (ε''_{eff}) shifts to lower frequency with increase in inclusion volume fraction. This shift in the frequency of the ε''_{eff} peak to the lower frequencies for the bigger inclusions ($r > 0.3\,\mu m$) might be explained as follows. The dipole moments of the bigger and "heavier" inclusions start opposing the high-frequency variations at the lower frequencies than the inclusions of smaller sizes. At the same time, the peak value for ε''_{eff} increases as the size of the inclusion increases, and this is related to the enhanced total loss within the bigger inclusion. Also, there is a factor of loss (effective conductivity) contrast between the inclusion and the host phase. The effective conductivity of a BT inclusion with the Debye dependence under consideration, σ_i, is on the order of a few S/m in the frequency range of interest, as opposed to the conductivity of the host, σ_h, which is

frequency-independent and on the order of 10^{-7} S/m. Therefore, there is not much influence of the loss in the host phase upon the maximum loss frequency of the composite. However, if $\sigma_h / \sigma_i > 10^{-3}$, there is a substantial shift of the maximum loss peak to the lower frequencies.

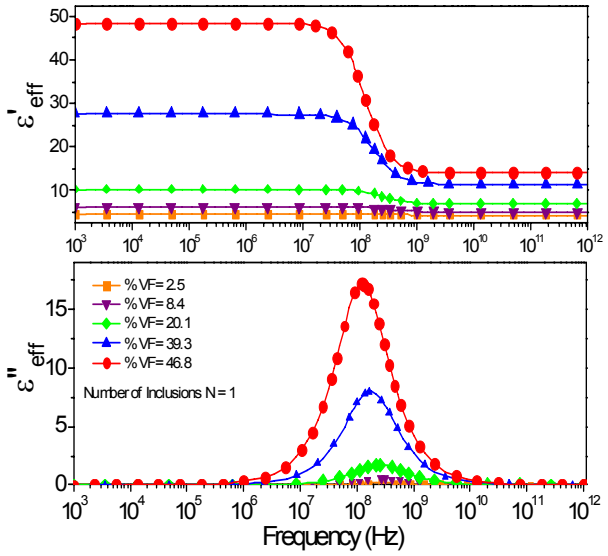

Figure 8. Prediction of effective permittivity of diphasic composite by equivalent impedance model for various inclusion volume fractions as a function of frequency.

These analytical equivalent impedance modeling results for spherical inclusions, as in Figure 8, were compared with numerical modeling results using the periodic finite-difference time-domain (FDTD) technique described in [37]. The FDTD results were obtained for a coarse mesh with $\Delta x = \Delta y = \Delta z = 0.044$ μm, while the total host cell had each side of 1.1 μm, similar to the setup in our analytical model. The results were compared for volume fractions of spherical inclusions of 46.8 % and 8.4 %, with identical BT and host phases. Figures 9 and 10 contain the extracted permittivity data using the FDTD technique. As is seen from the comparison, the results obtained using these two approaches agree reasonably.

The results of modeling using the equivalent impedance approach were also compared with modeling based on the Maxwell Garnett mixing rule. Figure 11 shows frequency dependencies of real and imaginary parts of permittivity for the same system with one inclusion in the host phase, modeled using Maxwell Garnett formulation.

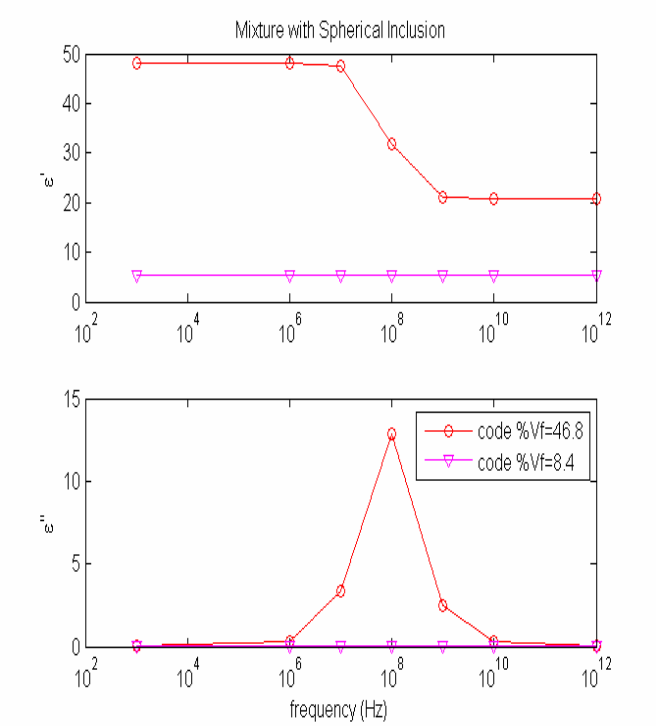

Figure 9. Prediction of effective permittivity of diphasic composite by FDTD numerical model [37] as a function of frequency for two different inclusion volume fractions.

It is seen that for the inclusion volume fraction of 46.8%, $\varepsilon'_{eff} \approx 14$ at 10^3 Hz, and it decreases to $\varepsilon'_{eff} \approx 13$ at $f = 10^{12}$ Hz, yielding a dielectric constant difference $\Delta\varepsilon_{eff} \approx 1$.

This demonstrates that the MG model is unable to accurately predict the frequency dependence of dielectric properties in mixtures with higher inclusion volume fractions. The MG model predictions considerably underestimate the effective permittivity of the composite.

The results of simulations, shown in Figure 8 can also be compared with the simulations based on the well-known logarithmic mixing rule. As is seen from Figure 12, the real part of permittivity predicted by the equivalent impedance model at 10^3 Hz is $\varepsilon'_{eff} \approx 71$, and decreases to ~29 at 10^{12} Hz, so that the difference $\Delta\varepsilon_{eff} = \varepsilon'_{eff\,s} - \varepsilon'_{eff\,\infty}$ is about 42.

The logarithmic mixing rule gives the static real permittivity value of approximately 1.5 times greater than that predicted by the equivalent impedance model for the inclusion volume fraction of 46.8%.

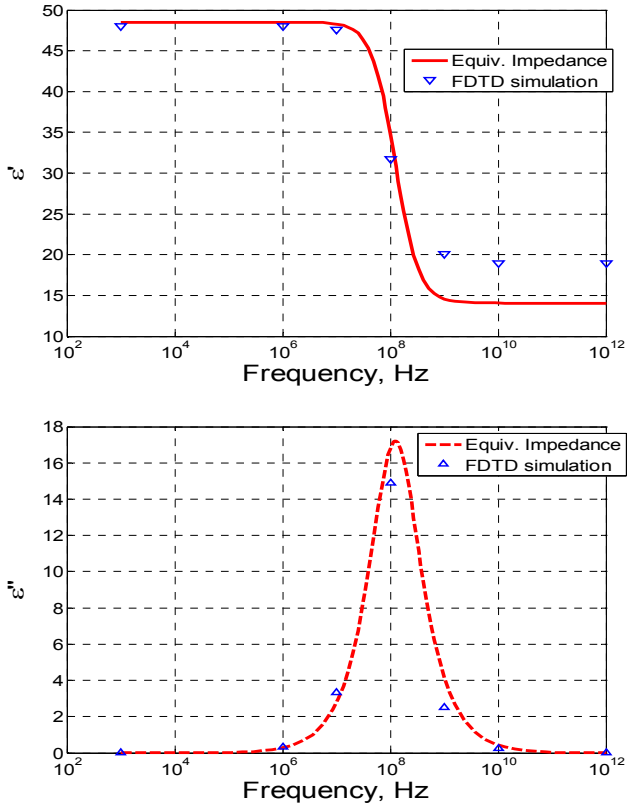

Figure 10. Comparison of equivalent impedance model and FDTD simulations for permittivity.

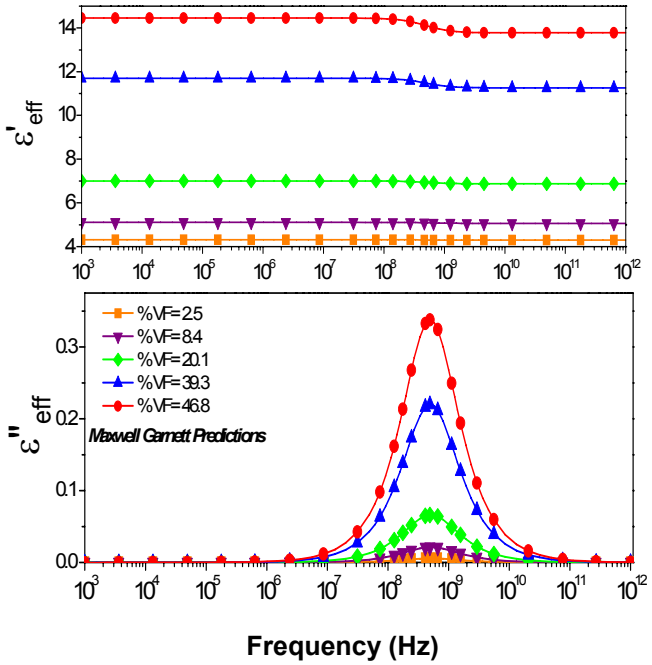

Figure 11. Prediction of the effective permittivity of a diphasic composite by Maxwell Garnett model for various inclusion volume fractions as a function of frequency.

The "optical" limit permittivity predicted by the logarithmic rule is about 2.5 times higher than in the equivalent impedance model for the same inclusion volume fraction. The discrepancy between the logarithmic mixing rule and the equivalent impedance model decreases as the inclusion volume fraction reduces. The results of computations based on both models almost coincide, when the inclusion volume fraction is less than 20%. At the same time, the Maxwell Garnett model agrees well with our model for the volume fraction of inclusions less than 10%. The logarithmic rule and Maxwell Garnett formulation and does not take into account shapes of inclusions, and multiple inclusions in three dimensions.

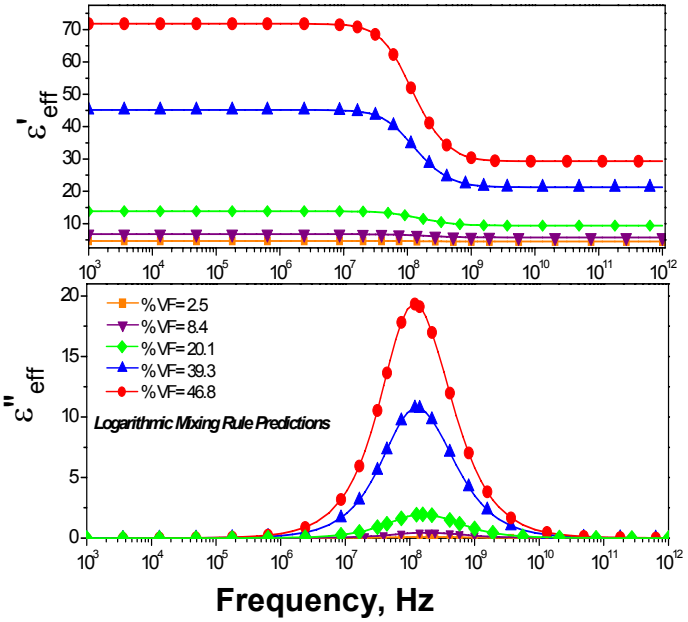

Figure 12. Effective permittivity of diphasic composite calculated using Logarithmic rule for various inclusion volume fractions.

The consistency of the equivalent impedance model for multiple inclusions in three dimensions has also been tested by studying a diphasic dielectric, but with N=1000 high-permittivity inclusions instead of a single one.

The maximum radius of each inclusion is 10 times smaller than in the previous example, and the inclusion volume fraction was held constant in both cases. In this particular case the inclusion size reduces and is varied from 10 nm to maximum 54.9 nm as opposed to the earlier case when single inclusion size was varied from 0.1 μm to a maximum of 0.549 μm. It has been verified that the equivalent impedance model for multiple smaller inclusions mathematically does not change compared to the single-inclusion prediction, as long as shape of inclusions and host cells remain the same. However, it is out of the scope of current research to be able to take into account extrinsic effects like particle size, temperature, electrode geometry, waveform of applied field, as well as electrical and thermal properties of electrodes. This research has primarily focused on studying the intrinsic attributes of diphasic composites system and evaluating their impact on effective permittivity through analytical modeling. All these extrinsic attributes have multiple

effects intertwined with other properties as well. For example, considering particle size, it should be pointed out that the permittivity of BT powder is highly sensitive to the grain size [38, 39], and it has been reported that coarse grain BT (20-50 μm) shows ε_r=1500…2000 at room temperature, whereas the permittivity for fine-grained BT (~1 μm) is 3500…4000. As the grain size decreases below 1 μm, the permittivity is most likely to be around 950…1200. However, it is worth mentioning that the effects due to a grain size (in a bulk body) and due to a particle size (isolated inclusion) may be different in the general case.

3.2. MIXTURE WITH CYLINDRICAL INCLUSIONS

Another example of a composite structure to be considered using the equivalent impedance method is a mixture of vertically aligned cylindrical high-permittivity inclusions in a low-permittivity host.

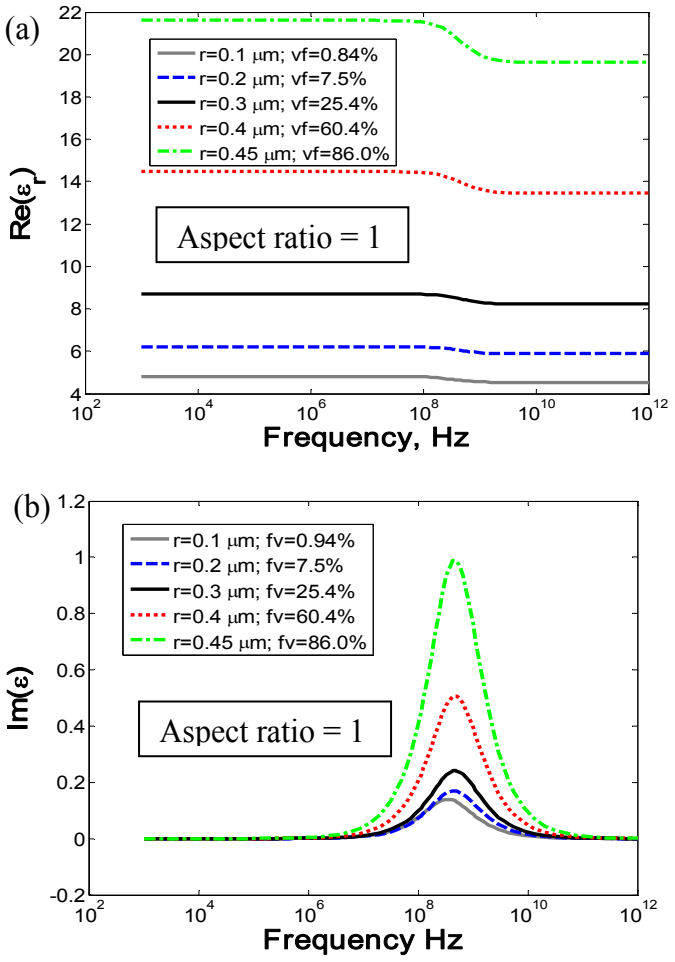

Figure 13. Real (a) and imaginary (b) parts of effective permittivity for a mixture of cylindrical inclusions with aspect ratio =1 at different radii (volume fractions) of inclusions.

Let us consider the same materials of phases as in the example with spherical inclusions. Static permittivity of inclusions is ε_{si}=1900, high-frequency permittivity is $\varepsilon_{\infty i}$=280, and the Debye constant is τ_i = 2.06 ns. The host has dielectric constant ε_h = 4, and an equivalent d.c. conductivity of σ_h=3.79·10^{-7} S/m.

Calculated frequency dependencies for composites with different sizes of inclusions (radii, aspect ratios, and corresponding volume fractions) are presented in Figures 13, 14, and 15. It is seen from these graphs that frequency dependencies of permittivity follow the Debye-type law (33). As radius of inclusions and the corresponding volume fraction increase, static values of effective permittivity also increase, and the loss peak becomes higher. These results agree well with those obtained in [40].

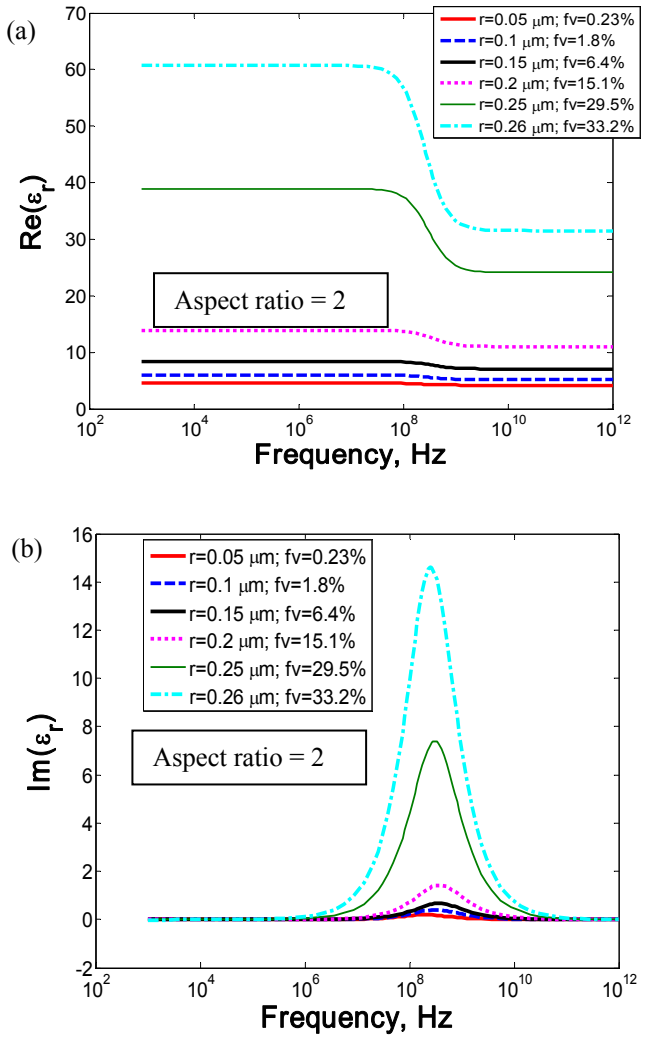

Figure 14. Real (a) and imaginary (b) parts of effective permittivity for a mixture of cylindrical inclusions with aspect ratio = 2 at different radii (volume fractions) of inclusions.

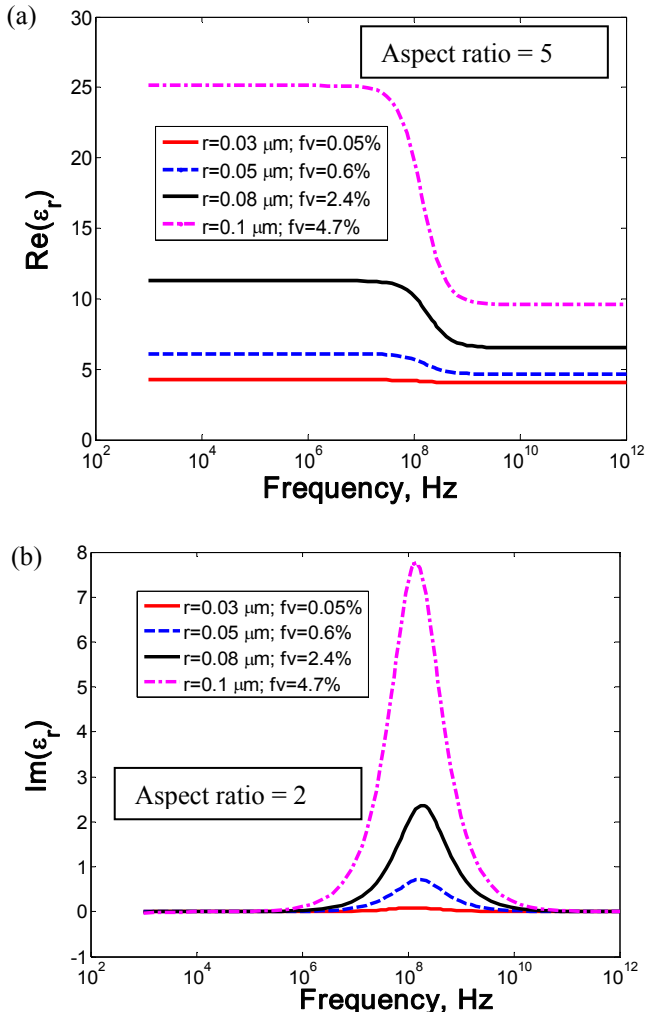

Figure 15. Real (a) and imaginary (b) parts of effective permittivity for a mixture of cylindrical inclusions with aspect ratio = 5 at different radii (volume fractions) of inclusions.

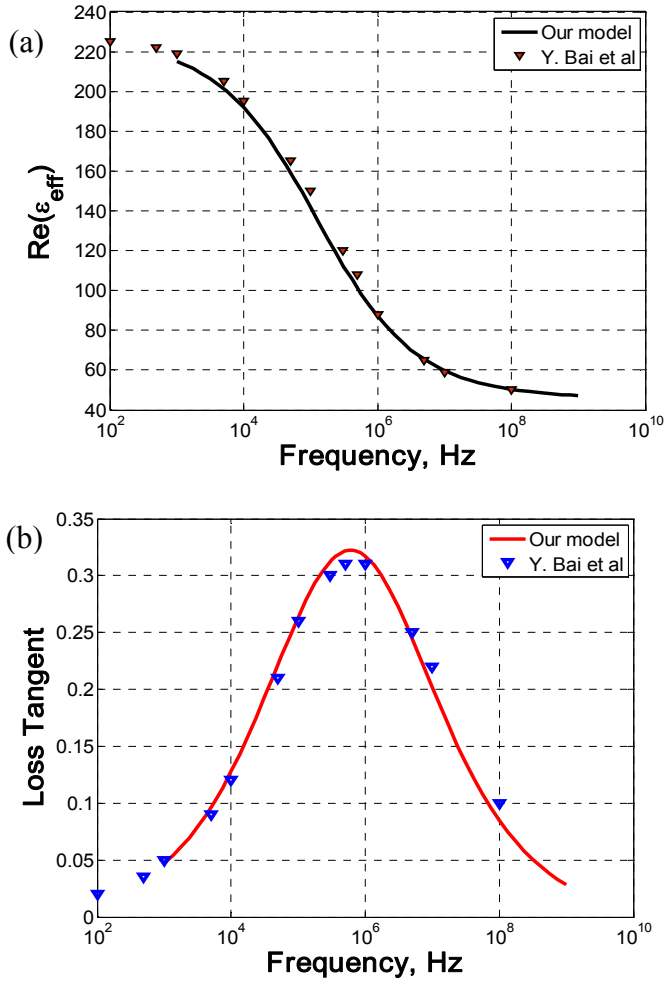

Figure 16. Real part of effective permittivity (a) and loss tangent (b) for a high-dielectric-constant ceramic-powder polymer composite – comparison with data in [47].

Aspect ratio significantly affects permittivity curves. It is seen that it is possible to achieve a higher static permittivity and corresponding loss peak when aspect ratio becomes higher, and this happens at much smaller inclusion volume fraction. In these simulations it is not allowed that two cylinders would touch, so maximum volume fraction of inclusions is determined by their aspect ratio.

This is a useful result from the point of view of developing materials with high permittivity, though not quite new, since this is an expected result. Similar phenomenon, *i.e.*, an increase of effective permittivity as aspect ratio of inclusions increases, has been studied in composites with conducting sticks [41-43], and also with dielectric rods [44, 45]. The calculations based on our model agree well with those published in literature – both numerical and experimental [46, 47].

3.3. COMPARISON OF MODELING WITH SOME EXPERIMENTAL RESULTS

The equivalent impedance model presented herein has been applied to simulate some published results available from experiment. The ceramic that was studied was PMN-PT (Pb-Mg-Nb – $PbTi0_3$) powder with an average particle diameter of 0.5 μm, and the host was P(VDF-TrFE) copolymer matrix, as reported in [47]. Frequency dependencies for dielectric constant and loss tangent of this composite at different temperatures were measured. The typical measuring method up to 1 GHz is based on application of impedance analyzers [48]. The measured data for 22 ^{0}C [47, Fig. 4] was compared with simulations based on the equivalent impedance approach. In this simulation, the Cole-Cole model was adopted for ceramic inclusions, rather than the Debye model.

$$\varepsilon_i(\omega) = \varepsilon_{\infty i} + \frac{\varepsilon_{si} - \varepsilon_{\infty i}}{1 + (j\omega\tau_i)^s} \qquad (28)$$

PMN-PT bulk ceramic with low porosity is known to have an outstanding static permittivity, which may be on the order of ~ 30,000 [49]. In these computations, the power s =0.484 (the same as in [47]), ε_{si} =11,000, $\varepsilon_{\infty i}$ =1,000, and τ_i =5.2 μs. At the same time, the host matrix was modeled using the Debye dependence with ε_{sh} =7.0, $\varepsilon_{\infty h}$ =4.5, and τ_h =1.8 ps. Figures 16a and 16b contains measured data taken from [47, Figure 4] and our simulated results.

4 CONCLUSIONS

The equivalent impedance circuit model for estimating the effective permittivity of a composite mixture as function of frequency was presented in this paper. The equivalent impedance model is simple solution to a complex problem and is able to take into account any inclusion shape and can predict dielectric permittivity and dielectric loss as a function of frequency.

This model is based on discretizing a dielectric body into partial impedance elements. The discretization process uniquely takes into account any inclusion size and shape. An RC-circuit analogy was used to account for loss in this model by assigning partial conductances along with the partial capacitances.

The model addressed in this paper is applicable to a periodic system consisting of high-permittivity spherical or cylindrical inclusion(s) enclosed in a cube with a lower permittivity phase. The model can be applied to any smooth-surface inclusions that could be discretized as slices. This approach can be further adopted by numerical electromagnetic techniques that deal with dispersive composite media that could be modeled as periodic disposition of inclusions in a host matrix.

In the particular cases studied in this paper, the complex permittivity of the equivalent impedance model showed the relaxation nature that could be approximated by Debye or Cole-Cole dependencies. However, in the general case, frequency characteristics of a composite depend on partial frequency responses of constituents, and may be either of the relaxation (RC-circuit analogy), or of resonance, narrowband or wideband Lorentzian (RLC-circuit analogy) behavior [50].

The equivalent impedance model was compared to Maxwell Garnett theory and Logarithmic mixing rule, FDTD numerical modeling permittivity extraction, and some published experimental results. It was shown that the Maxwell Garnett model considerably underestimates effective parameters predictions, especially for composites with volume fraction of inclusions greater than 20%. The logarithmic law, on the contrary, substantially overestimates the effective permittivity. Numerical simulation results and equivalent impedance model agree well and lie between the Maxwell Garnett (lower bound) and logarithmic law (upper bound) estimations.

As for limitations of the model, it is valid only in a quasistatic approximation, when any phase is considered in terms of lumped-element circuit analogy. Retardation, propagation, and multiple scattering effects are out of scope of this model.

This paper deals only with linear dielectrics, for which analysis in terms of frequency characteristics and circuit analogy is straightforward, since linear dielectrics behave as linear filters. Real and imaginary parts of permittivity satisfy Kramers-Kroenig relations for causality and passivity, analogous to Hilbert transform relations for linear passive circuits. However, the approach can be generalized for non-liner dielectrics as well, if their characteristics could be linearized locally in a "small-signal" regime. The approach can be also generalized for non-passive materials, if negative loss is modeled. It is also possible to extend this approach to consider random disposition of inclusions in a host material. However, these would be topics for separate papers.

ACKNOWLEDGEMENTS

Authors would like to kindly acknowledge the help of Dr. Wei Li in going through some of the details of the mathematical foundation of the work. This work was supported through a MURI program sponsored by the Office of Naval Research under Grant No. N000-14-05-1-0541, and also partially funded by the MS&T Consortium on Electromagnetic Compatibility.

APPENDIX

Calculation of the Corner Resistance

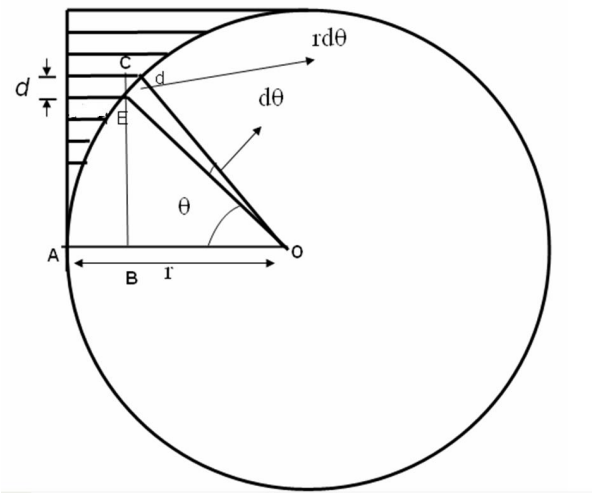

Figure 17. Vertically cut section of the inclusion sphere and corners detailing the discretization process for calculating the corner capacitance value.

Consider the corner resistor elements, as shown in Figure 17.

The area of the discretized corner plate for calculating corner resistances can be calculated from the Figure 18 as

$$S = 2r^2 - \frac{\pi \cdot r^2 \cos^2\theta}{2} \tag{A1}$$

From the triangle Δ EDO, the length ED is

$$l(ED) = r \cdot \sin(d\theta) \tag{A2}$$

As the angle $d\theta$ is very small,

$$l(ED) \approx r d\theta \tag{A3}$$

From the triangle ΔECD, the thickness d of any discretized plate can be found as

$$d = l(EC) = r\cos\theta \cdot d\theta \tag{A4}$$

The resistance is derived as follows.

$$dR_i = \frac{r\cos\theta \cdot d\theta}{\sigma_h\left[2r^2 - \frac{\pi \cdot r^2\cos^2\theta}{2}\right]} \tag{A5}$$

or

$$dR_i = \frac{2d(\sin\theta)}{r^2\sigma_h\left[(4-\pi)+\pi\sin^2\theta\right]} \tag{A6}$$

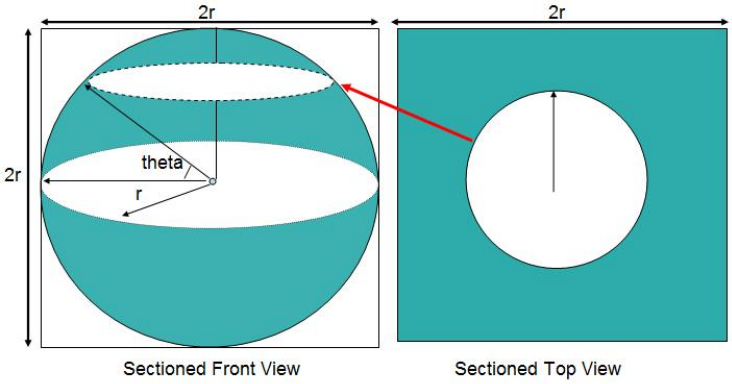

Figure 18. Sectional front and top view of the inclusion sphere and corner elements to illustrate the mathematics of the discretization process.

Substituting $x = \sin\theta$ into equation (B6), one can get

$$R_{ci} = \frac{2}{r\sigma_h\pi}\int_0^1 \frac{dx}{\frac{(4-\pi)}{\pi} + x^2} \tag{A7}$$

After integrating, the final expression for the corner resistance is obtained,

$$R_{ci} = \frac{2}{r\sigma_h\pi} \cdot \frac{1}{\sqrt{(\frac{4}{\pi}-1)}} \arctan\left[\frac{1}{\sqrt{(\frac{4}{\pi}-1)}}\right] = \frac{1.326}{r\sigma_h} \tag{A8}$$

REFERENCES

[1] J.C. Maxwell, *Electricity and Magnetism*, vol. 1, Clarendon Press, Oxford, UK, 1892.

[2] L.K.H. van Beck, "Dielectric behavior of heterogeneous systems", Ch. 3 in *Progress in Dielectrics*, vol. 7, J.B. Birks, ed., London, UK, Heywood Books, 1967.

[3] K. Lichtenecker, "Die Dielektrizitätkonstante natürlicher und künstlicher Mischkörper", Physikalische Zeitschrift, Vol. 27, No. 4/5, pp. 115-158, 1926.

[4] S. P. Mitoff, in *Advances in Materials Research*, edited by H. Herman (Wiley-Interscience, New York), Vol. 3, pp. 305–329, 1968.

[5] A. H. Sivhola, "How strict are theoretical bounds for dielectric properties of mixtures?", IEEE Trans. Geosci. Rem. Sens., Vol. 40, No. 4, pp. 880- 886, 2002.

[6] V. Myroshnychenko and C. Brosseau, "Finite-element modeling method for the prediction of the complex effective permittivity of two-phase random statistically isotropic heterostructures", J. Appl. Phys, Vol. 97, 044101-14, 2005.

[7] T.C. Choy, *Effective Medium Theory, Principles and Applications,* Oxford University Press, Oxford, UK, 1999.

[8] G.W. Milton, *Theory of Composites,* Cambridge University Press, Cambridge, UK, 2002.

[9] A.H. Sihvola, *Electromagnetic Mixing Formulas and Applications,* IEEE Publishing, London, UK, 1999.

[10] J.C. Maxwell Garnett, "Colours in metal glasses and in metallic films," Trans. of the Royal Society, London, UK, Vol. CCIII, pp. 385-420, 1904.

[11] R. Landauer, "Electrical conductivity in inhomogeneous media", in Electrical Transport and Optical Properties of Inhomogeneous Media, AIP Conf. Proc., edited by J. C. Garland and D.B. Tanner, New York, USA, Vol. 40, pp. 2-45, 1978.

[12] D. J. Bergman and D. Stroud, "Physical properties of macroscopically inhomogeneous media", Solid State Phys., Vol. 46, pp. 147-269, 1992.

[13] A. Spanoudaki, R. Pelster, "Effective dielectric properties of composite: The dependence on the particle size distribution", *Phys. Rev. B*, Vol. 64, 064205, 2001.

[14] M. Y. Koledintseva, J. Wu, J. Zhang, J. L. Drewniak, and K. N. Rozanov, "Representation of permittivity for multi-phase dielectric mixtures in FDTD modeling", IEEE Symp. Electromag. Compat. Santa Clara, CA, USA, Vol. 1, pp.309-314, 2004.

[15] J. Avelin and A. Sihvola, "Polarizability of polyhedral dielectric scatterers", Micro. Opt. Technol. Lett., Vol. 32, pp. 60-64, 2002.

[16] D. Payne, *The Role of Internal Boundaries upon the Dielectric properties of Polycrystalline Ferroelectric Materials*, Ph.D. Thesis, The Pennsylvania State University, USA, 1973.

[17] K. Wakino, T. Okada, N. Yoshida, and K. Tomono, "A New Equation for Predicting the Dielectric Constant of a Mixture", J. Am. Ceram. Soc., Vol. 76, pp. 2588-2594, 1993.

[18] C. Brosseau and A. Beroual, "Computational electromagnetics and the rational design of new dielectric heterostructures", Prog. Mater. Sci., Vol. 48, No. 5, pp. 373-456, 2003.

[19] C. Ang, Z. Yu, R. Guo, and A. Bhalla, "Calculation of dielectric constant and loss of two-phase composites", J. Appl. Phys., Vol. 93, pp. 3475-3480, 2003.

[20] A.H. Sihvola, and K.I. Nikoskinen, "Effective permittivity of mixtures: numerical validation by the FDTD method", IEEE Trans. Geoscience Remote Sens., Vol. 38, No. 3, pp. 1303-1308, 2000.

[21] B. Sareni, L. Krähenbühl, A. Beroual, and C. Brosseau, "Effective dielectric constant of periodic composite materials", J. Appl. Phys., Vol. 80, pp. 1688-1696, 1996.

[22] S.K. Patil and R. W. Schwartz, "Modeling Field Distribution and Energy Storage in Diphasic Dielectrics", 12th US-Japan Seminar on Dielectric & Piezoelectric Ceramics, Annapolis, MD, USA, 2005, pp. 397 – 400.

[23] B. Sareni, L. Krähenbühl, A. Beroual, and C. Brosseau, "Effective dielectric constant of random composite materials", J. Appl. Phys., Vol. 81, No. 5, pp. 2375-2383, 1997.

[24] B. Sareni, L. Krähenbühl, A. Beroual, and C. Brosseau, "Complex effective permittivity of a lossy composite material", IEEE Conf. Electr. Insul. Dielectr. Phenomena (CEIDP), Vol. 1, pp. 204-207, 1996.

[25] M.-J. Pan, B.A. Bender, and E.P. Gorzkowski, "Complex Permittivity Model of Barrier Layer Capacitor with Bimodal Grain Size Distribution", 12th US-Japan Seminar on Dielectric and Piezoelectric Ceramics, Annapolis, MA, USA, pp. 321-324, 2005.

[26] Y. Bai, Z. Y. Cheng, V. Bharti, H. S. Xu, and Q. M. Zhang, "High-dielectric-constant ceramic-powder polymer composites", Appl. Phys. Lett., Vol. 76, no. 25, pp. 3804-3806, 2000.

[27] M. Dang, Y. Shen, and C. W. Nan, "Dielectric behavior of three-phase percolative Ni–$BaTiO_3$/polyvinylidene fluoride composites", Appl. Phys. Lett., Vol. 81, No. 25, pp. 4814-4816, 2002.

[28] Y. Rao, J. M. Qu, T. Marinis, and C. P. Wong, "A precise numerical prediction of effective dielectric constant for polymer-ceramic composite based on effective-medium theory", IEEE Trans. Compon. Packag. Technol., Vol. 23, No. 4, pp. 680-683, 2000.

[29] Y. Rao, A. Takahashi, and C. P. Wong, "Di-block copolymer surfactant study to optimize filler dispersion in high dielectric constant polymer-ceramic composite", Composites, Part A: Applied Science and Manufacturing, pp. 1113-1116, 2003.

[30] C.J. Dias and D.K. Das-Gupta, "Inorganic ceramic/polymer ferroelectric composite electrets", IEEE Trans. Dielectr. Electr. Insul., Vol. 3, pp. 706–734, 1996.

[31] S.A. Tretyakov, F. Mariotte, C.R. Simovski, T.G. Kharina, and J.-P. Heliot, "Analytical antenna model for chiral scatterers: comparison with numerical and experimental data", IEEE Trans. Antennas and Propagat., Vol. 44, pp. 1006-1014, 1996.

[32] S.Tretyakov, *Analytical Modeling in Applied Electromagnetics*, Artech House, Chapters 5 and 6, 2003.

[33] S.K. Patil, M.Y. Koledintseva, W. Huebner, R. W. Schwartz, "Prediction of effective permittivity of diphasic dielectrics using an equivalent capacitance model", J. Appl. Phys., Vol. 104, 074108, 2008.

[34] M.P. McNeal, S.J. Jang, and R. Newnham, "The effect of grain and particle size on the microwave properties of barium Titanate", J. Appl. Phys., Vol. 83, no. 6, pp. 3288-3297, 1998.

[35] A.J. Moulson and J.M. Herbert, 2nd ed., *Electroceramics: Materials, Properties, Applications,* John Wiley & Sons, 2003.

[36] A. von Hippel," Piezoelectricity, ferroelectricity and crystal structure", Zeitschrift für Physik, Vol. 133, No. 1-2, pp. 158-173, 1952.

[37] D. Wu, R. Qiang, J. Chen, C. Liu, M. Koledintseva, J. Drewniak, and B. Archambeault, "Numerical modeling of periodic composite media for electromagnetic shielding applications", IEEE Symp. Electromag. Compat., Honolulu, Hawaii, USA, pp. 1-5, 2007.

[38] T.J. Lewis, "Interfaces are dominant feature of dielectrics at nanometer level", IEEE Trans. Dielectr. Electr. Insul., Vol. 11, pp. 739-753, 2004.

[39] G. Arlt, D. Hennings, and G. de With, "Dielectric properties of fine-grained barium titanate ceramics", J. Appl. Phys., Vol. 58, pp. 1619-1625, 1985.

[40] A. Beroual and C. Brosseau, "Comparison of dielectric properties determined from a computational approach and experiment for anisotropic and periodic heterostructures", IEEE Trans. Dielectr. Electr. Insul., Vol. 8, pp. 921-929, 2001.

[41] A. N. Lagarkov, S. M. Matytsin, K. N. Rozanov, A. K. Sarychev, "Dielectric Properties of Fiber-Filled Composites", J. Appl. Phys, Vol. 84, No. 7, pp. 3806-3814, 1998.

[42] S.M. Matitsine, K.M. Hock, L.Liu, Y.B. Gan, A.N. Lagarkov, and K.N. Rozanov, "Shift of resonance frequency of long conducting fibers embedded in a composite", J. Appl. Phys., Vol. 94, pp. 1146-1154, 2003.

[43] M.Y. Koledintseva, R.E. DuBroff, and R.W. Schwartz, "A Maxwell Garnett model for dielectric mixtures containing conducting particles at optical frequencies", Progress in Electromagnetic Research (PIER), Vol. 63, pp. 223-242, 2006.

[44] C. Brosseau, A. Beroual, and A. Boudida, "How do shape anisotropy and spatial orientation of the constituents affect the permittivity of dielectric heterostructures?", J. Appl. Phys., Vol. 88, pp. 7278-7288, 2000.

[45] A. Beroual, C. Brosseau, and A. Boudida, "Permittivity of lossy heterostructures: effect of shape anisotropy", J. Phys. D: Appl. Phys., Vol. 33, No. 16, pp. 1969-1974, 2000.

[46] C. Brosseau and A. Beroual, "Computational electromagnetics and the rational design of new dielectric heterostructures", Progress in Materials Science, Vol. 48, pp. 373-456 2003.

[47] Y.Bai, Z.-Y. Cheng, V. Bharti, H.S. Xu, and Q.M. Zhang, "High-dielectric-constant ceramic-powder polymer composites", Appl. Phys. Lett., Vol. 76, pp. 3804-3806, 2000.

[48] H. Kakemoto, J. Li, S.M. Nam, S. Wada, and T. Tsurumi, "Dielectric spectra of $BaTi0_3$ materials measured by impedance analyzer up to 1 GHz", Jpn. J. Appl. Phys., Vol. 42, Part 1, No. 9B, pp. 6143-6148, 2003.

[49] M.R.Cox, "Large diameter high performance PMN-PT 90/10 ceramic produced by hot pressing", J. Mater. Science Lett., Vol. 19, pp. 333-334, 2000.

[50] M.Y.Koledintseva, J.L.Drewniak, D.J.Pommerenke, K.N. Rozanov, G.Antonini, and A.Orlandi, "Wideband Lorentzian media in the FDTD algorithm", IEEE Trans. Electromag. Compat., Vol. 47, No.2, pp. 392-398, 2005.

Marina Y. Koledintseva (M'96-SM'03) received the M.S. degree (with excellence) in 1984 and Ph.D. degree in 1996 from Radio Engineering Department of Moscow Power Engineering Institute (Technical University)– MPEI(TU), Moscow, Russia. In 1983-1999 she worked with the Ferrite Laboratory of MPEI (TU), and in 1997-1999 she combined research with teaching as an Associate Professor in the same University. In January 2000, she came to the USA as a Visiting Professor and joined the EMC Laboratory of the Missouri University of Science and Technology (MS&T), formerly known as the University of Missouri-Rolla. Since 2005 she has been a Research Professor in MS&T. Her scientific interests are microwave engineering, interaction of electromagnetic field with ferrites, dielectrics, and composite media, their modelling, and application for electromagnetic compatibility. She has published over 150 papers, and is an author of 7 patents. Currently, Dr. Koledintseva is a member of TC-9 (Computational Electromagnetics), TC-11 (Nanotechnology), and TC-4 (Shielding) Committees of the IEEE EMC Society.

Sandeep Patil was born in Jalgaon, India in 1980. He received the B.E degree from the Government College of Engineering, Pune, India in 2001, the MS degree in Ceramic Science and Engineering in 2003 and the Ph.D. degree from Missouri University of Science and Technology (formerly known as University of Missouri-Rolla), USA in 2008 in Materials Science and Engineering. Dr. Patil is currently working as Senior Technology Development Engineer at Intel Corporation, Portland USA. Sandeep's research interest include dielectric composites, ferroelectrics, thin films and glass ceramic dielectrics and integrated circuit manufacturing.

Robert W. Schwartz is Vice Provost for Academic Affairs at the Missouri University of Science and Technology (Missouri S&T). His research interests include piezoelectric composites, dielectric materials and the chemical synthesis of electronic ceramics. Schwartz was previously employed as Professor of Materials Science and Engineering at Missouri S&T, Associate and Assistant Professor of Materials Science and Engineering at Clemson University, Senior Member of the Technical Staff at Sandia National Laboratories, and Research Engineer at B. F. Goodrich. Schwartz received his B.S. in science education and his M.S. in chemistry, both from North Carolina State University. He received his Ph.D. in ceramic engineering from the University of Illinois, Urbana, Illinois, in 1989. Schwartz is the holder of two U. S. patents, has published more than 100 papers, and has authored six book chapters. Schwartz is a member of the Institute of Electrical and Electronic Engineers, the American Ceramic Society, the Materials Research Society, and the American Society of Engineering Educators. Schwartz is a Fellow of the American Ceramic Society. He currently serves as the General Secretary of Keramos, the National Ceramic Engineering Fraternity, and is Past Chair of the Electronics Division of the American Ceramic Society.

Jianxiang Shen was born in Shandong Province, China, in 1984. He received the B.S. degree in Electrical Engineering from Ocean University of China, Qingdao, China, in 2006, and is currently working toward the Ph.D. degree at University of Houston, Houston, TX. His research interests include computational electromagnetic, stochastic analysis, and the design/analysis of periodic structures.

Wayne Huebner is a Professor of Ceramic Engineering, and the Chairman of the Materials Science and Engineering Department at the Missouri University of Science & Technology in Rolla, Missouri. He began his academic career as an Assistant Professor at the Pennsylvania State University, and moved back to S&T in 1991. The author of over 85 papers, monographs and book chapters, he has been actively involved in the preparation and characterization of electronic ceramics. Much of his research is focused on the use of dielectrics, ionic and mixed conductors, piezoelectrics, electrostrictive materials for multilayer capacitors, solid oxide fuel cells, gas separation membranes, and phased linear array transducers for intravascular imaging. He has graduated 9 Ph.D. students and 14 M.S. students. Huebner has received S&T's Faculty Excellence Award five times, the Outstanding Teacher Award four times, and was named the Outstanding Faculty Member in Ceramic Engineering five consecutive years. He has been a continuous member of the Electronics Division of American Ceramic Society since 1983, serving in many capacities including all offices of the Ceramic Educational Council, an organizer of various symposia, and Associate Editor of the Journal of the ACS.

Konstantin Rozanov was born in Moscow, Russia, in 1960. He received a degree from Moscow State University, Russia, in 1983, and the Ph.D. degree in electrical engineering from the Institute for High Temperatures, Russian Academy of Sciences, Moscow, Russia, in 1991. Since 1986, he has been with the Scientific Center for Applied Problems in Electrodynamics (SCAPE) of Russian Academy of Sciences, Moscow, Russia, which was renamed the Institute of Theoretical and Applied Electromagnetics (ITAE) in 1999. Since 1997, he has been Head of the Microwave Laboratory of SCAPE/ITAE, where he is involved in research dealing with microwave properties of composites, microwave magnetic materials, microwave measurement techniques, radar absorbers, and RCS reduction. His current personal research interests include design and characterization of microwave absorbers and frequency selective surfaces, free-space microwave measurement methods, frequency dispersion of permittivity and permeability, and properties of composites and complex media.

Ji Chen (S'87-M'90-SM'07) received the Bachelor's degree from Huazhong University of Science and Technology, Wuhan, Hubei, China, the Master's degree from McMaster University, Hamilton, ON, Canada, in 1994, and the Ph.D. degree from the University of Illinois at Urbana-Champaign in 1998, all in electrical engineering. He is currently an Associate Professor with the Department of Electrical and Computer Engineering, University of Houston, Houston, TX. His research interests include computational electromagnetic, modeling and design of biomedical instruments, stochastic analysis of periodic structure and non-periodic structures, and characterization of composite materials. Prior to joining the University of Houston, from 1998 to 2001, he was a Staff Engineer with Motorola Personal Communication Research Laboratories, Chicago, IL. Dr. Chen has received outstanding teaching award and outstanding junior faculty research award from College of Engineering at University of Houston. He is also the recipient of ORISE fellowship in 2007. His research group also received the best student paper award at IEEE EMC Symposium 2005 and the best paper award from IEEE APMC conference in 2008.